ChemPubSoc Europe

DOI: 10.1002/chem.201503490

CHEMISTRY A European Journal Full Paper

Acceptor–Donor Conjugates |*Hot Paper*|

Engaging Copper(III) Corrole as an Electron Acceptor: Photoinduced Charge Separation in Zinc Porphyrin–Copper Corrole Donor–Acceptor Conjugates

Thien H. Ngo,*[a, b] David Zieba,[c] Whitney A. Webre,[d] Gary N. Lim,[d] Paul A. Karr,[e] Scheghajegh Kord,[c] Shangbin Jin,[b] Katsuhiko Ariga,[b] Marzia Galli,[f] Steve Goldup,[f] Jonathan P. Hill,*[b] and Francis D'Souza*[d]

Abstract: An electron-deficient copper(III) corrole was utilized for the construction of donor–acceptor conjugates with zinc(II) porphyrin (ZnP) as a singlet excited state electron donor, and the occurrence of photoinduced charge separation was demonstrated by using transient pump–probe spectroscopic techniques. In these conjugates, the number of copper corrole units was varied from 1 to 2 or 4 units while maintaining a single ZnP entity to observe the effect of corrole multiplicity in facilitating the charge-separation process. The conjugates and control compounds were electrochemically and spectroelectrochemically characterized. Computational studies revealed ground state geometries of the compounds and the electron-deficient nature of the copper(III) corrole. An energy level diagram was established to predict the photochemical events by using optical, emission, electrochemical, and computational data. The occurrence of charge separation from singlet excited zinc porphyrin and charge recombination to yield directly the ground state species were evident from the diagram. Femtosecond transient absorption spectroscopy studies provided spectral evidence of charge separation in the form of the zinc porphyrin radical cation and copper(II) corrole species as products. Rates of charge separation in the conjugates were found to be of the order of $10^{10}\ s^{-1}$ and increased with increasing multiplicity of copper(III) corrole entities. The present study demonstrates the importance of copper(III) corrole as an electron acceptor in building model photosynthetic systems.

Introduction

Increasing global energy demands and environmental concerns due to burning fossil fuels have given energy research a high priority in recent years.[1] In this regard, energy-harvesting materials, especially those that mimic natural photosynthesis, have attracted much attention owing to their potential capabilities for direct conversion of incident light to an electrical current, which makes them a useful power source.[2] Porphyrins have been commonly used as photosensitizers for the construction of artificial photosynthetic systems because of their resemblance to the naturally occurring chlorophyll pigments.[3] However, other sensitizers, including phthalocyanines,[4] corroles,[5] subphthalocyanines,[6] bodipy,[7] and structural isomers of porphyrins[8] have also been exploited for this purpose. Furthermore, in recent work, molecular engineering has been applied in the preparation of elegant multi-modular donor–acceptor systems that are capable of wide-band capture and of generating the long sought after long-lived charge-separated states upon photoexcitation.[9] The utilization of tribasic corroles in the construction of donor–acceptor systems has been a focus of attention in recent years because of their metal cation coordinative properties and other unique features that make them distinct from porphyrins, including easier oxidation.[10] Consequently, there already exist a few reports on

[a] *Dr. T. H. Ngo*
International Center for Young Scientist (ICYS)
National Institute for Materials Science
Namiki 1-1, Tsukuba, Ibaraki 305-0044 (Japan)
Fax: (+81) 298604832
E-mail: NGO.Huynhthien@nims.go.jp

[b] *Dr. T. H. Ngo, Dr. S. Jin, Dr. K. Ariga, Dr. J. P. Hill*
WPI Center for Materials Nanoarchitectonics
National Institute for Materials Science
Namiki 1-1, Tsukuba, Ibaraki 305-0044 (Japan)
Fax: (+81) 298604832
E-mail: Jonathan.Hill@nims.go.jp

[c] *D. Zieba, S. Kord*
Institut für Chemie und Biochemie, Freie Universität Berlin
Takustrasse 3, 14195 Berlin (Germany)

[d] *W. A. Webre, G. N. Lim, Prof. Dr. F. D'Souza*
Department of Chemistry, University of North Texas
1155 Union Circle, 305070, Denton, TX 76203 (USA)
Fax: (+1) 940-565-4318
E-mail: Francis.Dsouza@unt.edu

[e] *Prof. Dr. P. A. Karr*
Department of Physical Sciences and Mathematics
Wayne State College
111 Main Street, Wayne, NE, 68787 (USA)

[f] *M. Galli, Prof. Dr. S. Goldup*
Department of Chemistry, University of Southampton
Southampton, SO17 1BJ (UK)

Supporting information for this article is available on the WWW under http://dx.doi.org/10.1002/chem.201503490.

donor–acceptor dyads featuring corroles as the photosensitizer/electron donor.[5] However, application of corroles as electron acceptors has hardly been studied,[5i,j] primarily owing to the lack of a corrole or metallocorrole derivative with an appropriately facile reduction potential. The exception to this generalization is provided by the recently reported copper(III) corroles that are known to undergo facile reduction from copper(III) to copper(II).[11] In the majority of copper(III) corroles, the $Cu^{III/II}$ reduction potential is lower than that of the widely used electron acceptors such as fullerenes[12] and quinones.[13] In the present study, we have exploited this novel property of copper(III) corroles in the construction of covalently linked donor–acceptor dyads, triads, and pentads that use zinc(II) porphyrin (ZnP) as the electron donor.

Several corrole–porphyrin conjugates have been reported over the past ten years. Multistep sequential syntheses have been described by Paolesse, Smith, Zheng, and co-workers to afford directly unsymmetrical corrole–porphyrin dyads or those containing spacers with linkage through their *meso*-positions.[14–16] Also, Guilard, Kadish, and co-workers have described the electrochemistry, photophysics, and catalytic properties of several cofacial corrole–porphyrin hybrids containing different transition-metal cations.[17–26] Other synthetic pathways reported in the literature have involved the preparation of individual corrole and porphyrin moieties followed by their intermolecular linkage. Osuka and co-workers[27] reported the preparation of β,β-linked corrole dimers by using Suzuki–Miyaura cross-coupling (after regioselective Ir-catalyzed direct borylation), whereas Gryko has disclosed the preparation of a *meso–meso*-corrole–porphyrin dyad containing an amide and imide spacer.[28,29] In recent years, we have focused on the synthesis and functionalization of corrole.[30–38] One such example involves a high yielding preparation of a bis-porphyrin–corrole triad employing nucleophilic aromatic substitution of the pyrimidinyl-substituted corroles involving phenolic porphyrins.[30] The first report of the application of the click reaction in tetrapyrrole chemistry was made by Collman and Chidsey in 2006.[39] Recently, Le Pleux et al. described multiporphyrin arrays with different metal centers constructed by using the click reaction.[40] In this work, we describe an investigation of different corrole–porphyrin conjugates prepared by using the click reaction. The structures of the newly prepared donor–acceptor conjugates are shown in Figure 1 together with those of the control compounds.[41] Here, we report not only the high yielding synthesis of the porphyrin–corrole dyads, but also provide definitive spectroscopic evidence for the occurrence of photoinduced electron transfer within these conjugates. Covalent linkage of the different units was accomplished by using the well-known click chemistry involving formation of 1,2,3-triazole moieties.[42] Synthetic details are given in the Experimental Section and Supporting Information. The purity of the compounds was confirmed by thin layer chromatography whereas structures were confirmed by using ^{1}H and ^{13}C NMR, mass spectrometric, and spectroscopic studies. All compounds were ESR silent, indicating that copper corrole, CuC, exists as $Cu^{III}C$. Photoinduced electron transfer in these donor–acceptor conjugates was established and studied by using femtosecond transient absorption spectroscopy.

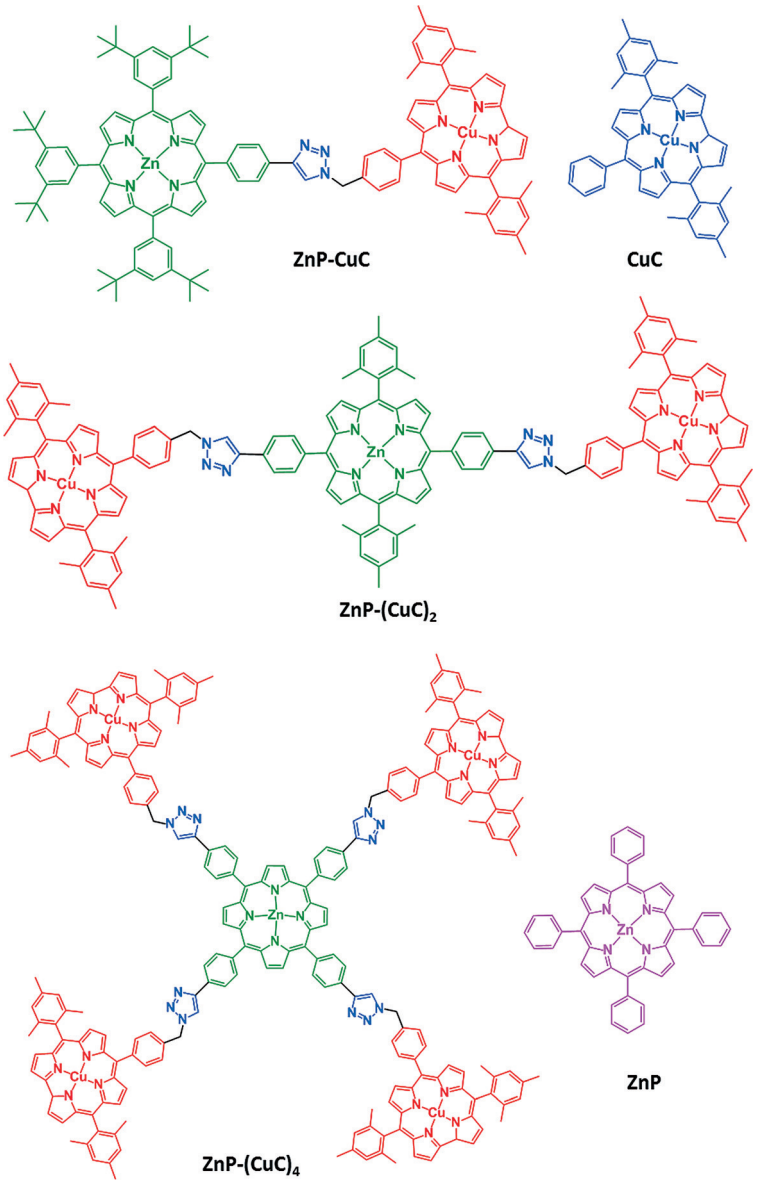

Figure 1. Structures of the zinc porphyrin–copper corrole donor–acceptor conjugates, and the control compounds investigated in the present study.

Results and Discussion

Synthesis

Four different reaction conditions were investigated in the optimization of the synthetic procedure for making the corrole–porphyrin conjugates from azidocorrole **1** and porphyrins **2–4**

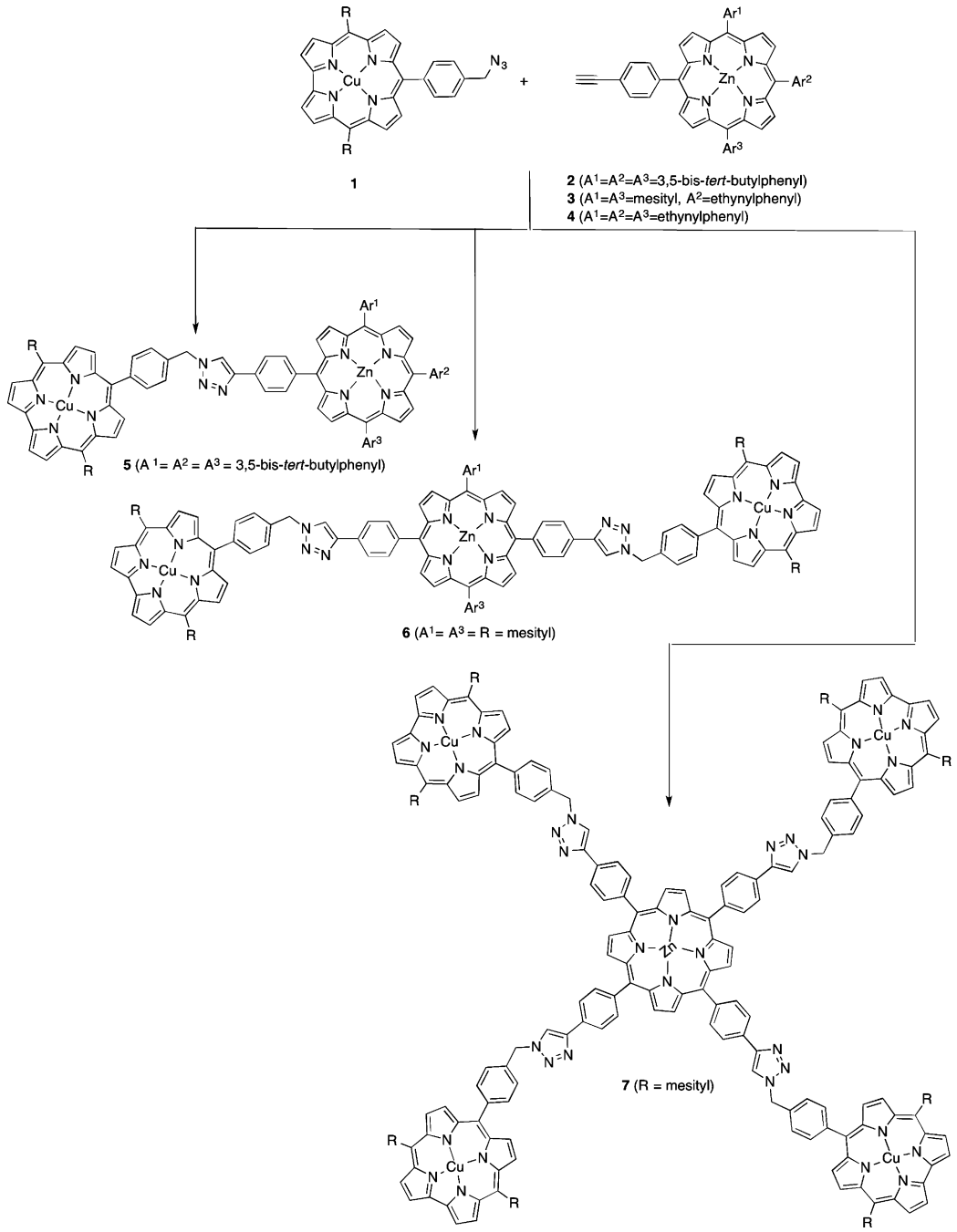

Scheme 1. Click synthesis of the conjugates **5**, **6**, and **7**.

(Scheme 1, Table 1). The active catalytic species for the coupling is Cu^{I}, which can be introduced directly by using Cu^{I} salts or by its in situ generation by reduction of Cu^{II}. Reactions were carried out in the presence of an excess of Cu–corrole **1** with the reaction monitored by using thin layer chromatography (TLC).

Dyad **5** was obtained in 88% yield when Cu^{I} was added directly in the form of CuI whereas yields as high as 94% could be obtained by employing the in situ formation of the Cu^{I} catalyst by reduction of copper(II) sulfate with ascorbic acid. Hu and Wang have described acid- and base-promoted click reac-

Table 1. Isolated yields [%] of conjugates **5**–**7** with different copper catalysts.

	Dyad **5**	Triad **6**	Pentad **7**
CuI[a]	88		
$CuSO_4 \cdot 5H_2O$/ascorbic acid[b]	94	89	79
CuI/DIPEA/acetic acid[c]	quantitative	73	63
$[Cu(CH_3CN)_4]PF_6$[d]	quantitative	99	98

[a] Acetonitrile, dichloromethane, RT, 3 d. [b] DMF, 50 °C, 3 d. [c] RT, 1 d, DIPEA = *N*,*N*-diisopropylethylamine. [d] Dichloromethane, 80 °C, 12–24 h.

tions.[44,45] By applying this procedure to our system, essentially quantitative yields could be obtained after 24 h. A similar result was obtained if tetrakis(acetonitrile)copper(I) hexafluorophosphate ($[Cu(CH_3CN)_4]PF_6$) was added as a catalyst. For the synthesis of triad **6** and pentad **7**, the reaction conditions with the three highest yields for the dyad were selected. The yields for the click reaction of copper corrole **1** and bis-acetylenyl porphyrin **3**, leading to triad **6**, were slightly lower than for the dyad at 89 and 73% for the in situ reduced $CuSO_4$ pentahydrate and acid–base mediated CuI catalyst, respectively. As expected, the yields from the same reaction were reduced further to 79 and 63%, respectively, for the preparation of pentad **7** from tetra-acetylenyl porphyrin **4** and azidocorrole **1**. $[Cu(CH_3CN)_4]PF_6$ gave the most satisfying results with no significant reduction in yield observed for **6** or **7**.

Absorbance and emission studies

Figure 2a shows the absorption spectra of representative compounds in benzonitrile. ZnP exhibits a Soret band at 428 nm, and bands in the visible range at 557 and 598 nm. The Soret band of CuC appears at 413 nm with broad spectral features in the visible range between 500–660 nm. The spectrum of a mixture of equivalent amounts of ZnP and CuC is similar to that of the ZnP–CuC dyad. The spectra of the triad and pentad were also simple additions of the spectra of the respective stoichiometric amounts of their individual components. These observations suggest a lack of significant intramolecular interactions between the entities. At 400 nm, the excitation wavelength of our femtosecond transient spectrometer, about 75% of the absorbance was due to CuC whereas about 25% was due to ZnP in the case of the dyad.

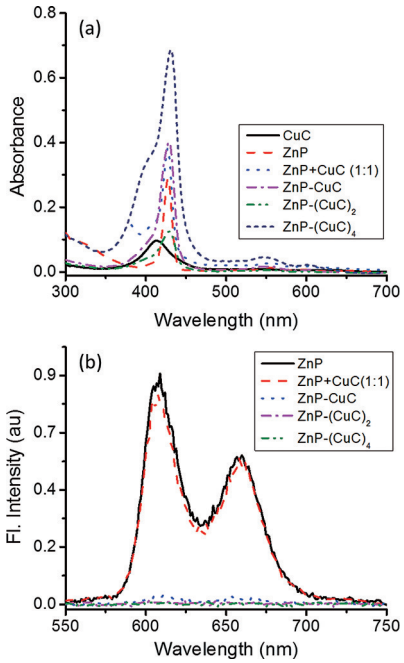

Figure 2. Electronic absorption and fluorescence spectra of the indicated compounds (and a mixture) in benzonitrile. Concentration was maintained at 2.5×10^{-6} M for all samples. $\lambda_{ex}=428$ nm.

Fluorescence spectra of the conjugates and the control compounds are shown in Figure 2b. The emission spectrum of ZnP contains peaks at 608 and 660 nm whereas CuC was non-fluorescent. ZnP emission was quenched by less than 5% when equimolar CuC was added to the solution, suggesting a lack of intermolecular association, which would lead to fluorescence quenching between the entities. Conversely, in the covalently linked conjugates, strong quenching was observed at 96% for ZnP–CuC, and over 99% in the case of ZnP–$(CuC)_2$ and ZnP–$(CuC)_4$. Varying the excitation wavelength from 428 nm to 557 nm of ZnP lead to similar spectral and quenching trends. These results suggest the occurrence of intramolecular events from the singlet excited state of ZnP (^{1}ZnP*) to CuC in the conjugates.

Electrochemical and spectroelectrochemical studies

Differential pulse voltammograms (DPVs) of the ZnP–CuC dyad along with control compounds (CuC and ZnP) are shown in Figure 3. The first reduction of $Cu^{III}C$ is located at −0.61 V versus Fc/Fc^+, indicating that it is nearly 400 mV easier to reduce than the other popular electron acceptors, C_{60} and benzoquinone,[12a,13a] signifying its potential as an electron acceptor in building donor–acceptor conjugates.

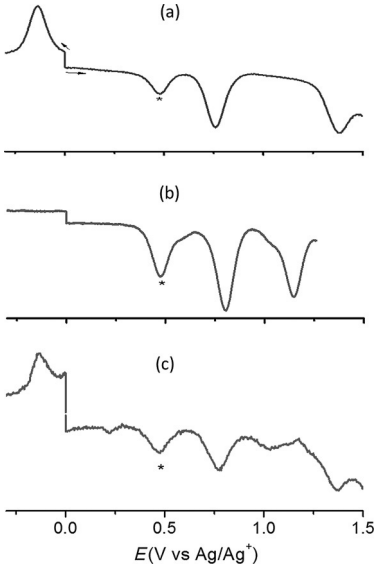

Figure 3. Differential pulse voltammograms of a) CuC, b) ZnP, and c) ZnP–CuC dyad in benzonitrile containing 0.1 M $(nBu_4N)ClO_4$. Scan rate = 20 mV s^{-1}, pulse width = 50 ms, pulse height = 0.025 V. The "*" corresponds to the oxidation of ferrocene used as an internal standard.

On the anodic side, two oxidations at 0.28 and 0.90 V versus Fc/Fc^+, corresponding to corrole ring oxidations, were observed (Figure 3a). ZnP, used as an electron donor in the present study, undergoes two oxidations at 0.32 and 0.67 V versus Fc/Fc^+, corresponding to ring oxidations (Figure 3b). The first

reduction of ZnP is located at −1.79 V versus Fc/Fc^+. In the ZnP–CuC dyad, the first reduction of CuC was found to be at the same potential of −0.61 V whereas the first oxidation process appears as an overlap of the first oxidations of ZnP and CuC, appearing at 0.30 V. Other anodic processes were at potentials not significantly different from the control compounds. Similar voltammograms were obtained for the triad and pentad, although the currents of the CuC redox couples were larger, as anticipated from the increased number of CuC entities (two in the case of the triad and four in the case of pentad).

Further spectroelectrochemical studies on the control compounds and donor–acceptor dyad were performed to characterize spectrophotometrically the one-electron oxidized and reduced species, which assists in the spectral interpretation of transient absorption data. The spectral changes observed for $Cu^{III}C$ reduction are typical of spectral changes associated with metal-centered reduction. During reduction, the Soret band located at 414 nm diminished in intensity with the appearance of a new band at 435 nm. In the visible region, new peaks at 577 and 610 nm were observed (see Figure S13a in the Supporting Information). Isosbestic points at 357 and 462 nm were observed and these spectral changes were found to be fully reversible. During the first oxidation of CuC, the 412 nm peak was diminished and redshifted to a broad peak centered at 421 nm. Isosbestic points at 381 and 434 nm were observed (Figure S13b).

Reduction of ZnP was accompanied by the appearance of new redshifted peaks at 438, 574, and 615 nm with these spectral changes being reversible (Figure S13c). During the first oxidation of ZnP, Soret and visible bands were diminished in intensity with the appearance of new peaks at 370, 454 (sh), 602, and 674 nm (br). These spectral changes were reversible with isosbestic points at 416, 438, and 543 nm (Figure S13d).

Next, the spectroelectrochemical study on the representative ZnP–CuC dyad was performed. As shown in Figure 4a for the first reduction, new peaks at 575 and 605 nm, which were similar to those observed during reduction of pristine CuC, were observed. This confirms formation of $ZnP–Cu^{II}C$ during the first electroreduction of the dyad. During the first oxidation, the typical blueshifted ZnP Soret band and broad spectral features in the 600–700 nm range characteristic of ZnP oxidation were observed (Figure 4b). This confirms formation of $ZnP^{\bullet+}$–CuC during electrooxidation of the dyad. Observation of these peaks during transient spectral studies would confirm photoinduced electron transfer leading to formation of the $ZnP^{\bullet+}$–$Cu^{II}C$ radical ion pair in these donor–acceptor conjugates.

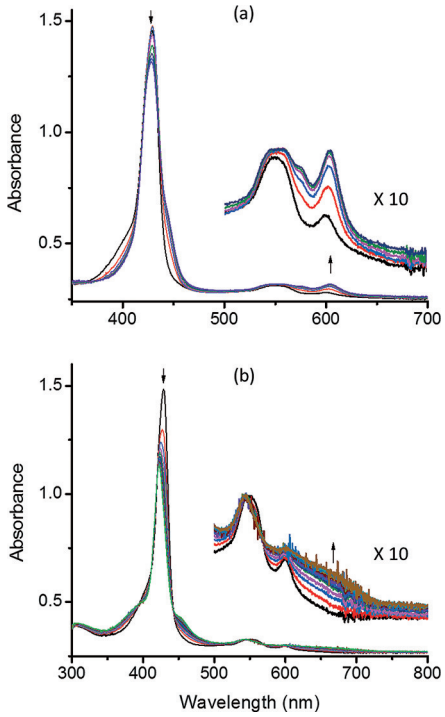

Figure 4. Spectral changes observed during a) first reduction and b) first oxidation of ZnP–CuC dyad in benzonitrile containing 0.1 M $(nBu_4N)ClO_4$.

Computational studies

The geometry and electronic structures of the conjugates were probed by using the B3LYP functional and a mixed basis set (H and C(6-31G), N and O(6-31G(d), and Cu and Zn(6-31G(df)) as parameterized in the Gaussian 09 software suite.[43] The ZnP and CuC entities were constructed by using the GaussView program on a local PC. After construction, the structures were uploaded to a supercomputer and then the geometry of both were optimized to a stationary point on the Born–Oppenheimer surface by using the model chemistry and software described above. Using the Gaussview program on a local PC, the optimized ZnP and CuC entities were then used to construct the dyad (compound a), the triad (compound b), and the pentad (compound c). Once constructed, the geometries of the dyad, triad, and pentad were uploaded to a supercomputer and optimized to a stationary point on the Born–Oppenheimer surface. Next, by using the GaussView program, frontier orbitals were generated for each of the optimized structures as shown in Figure 5. Symmetric disposition of the CuC entities around the central ZnP in the triad and pentad were observed.

The Cu–Zn distance in the optimized geometry of the dyad was approximately 17.6 Å, the edge-to-edge distance was approximately 10.19 Å, the Cu–triazole center distance was approximately 10.4 Å, and the Zn–triazole center distance was approximately 10.5 Å. The Cu–Cu distance in the optimized geometry of the triad was approximately 34.9 Å, the edge-to-edge distance was approximately 44.8 Å, the average Cu–Zn distance was approximately 9.86 Å, the average Cu–triazole center distance was approximately 10.4 Å, and the average Zn–triazole center distance was approximately 10.4 Å.

The average Cu–Cu distance of the "*cis*" Cu in the optimized geometry of the pentad was approximately 25.0 Å, the average Cu–Cu distance of the "*trans*" Cu was approximately 35.4 Å, the edge-to-edge distance was approximately 10.30 Å, the average Cu–Zn distance was approximately 17.7 Å, the average Cu–triazole center distance was approximately 10.5 Å, and the average Zn–triazole center distance was approximately 10.5 Å. Importantly, no steric crowding or constraints were found in these superstructures.

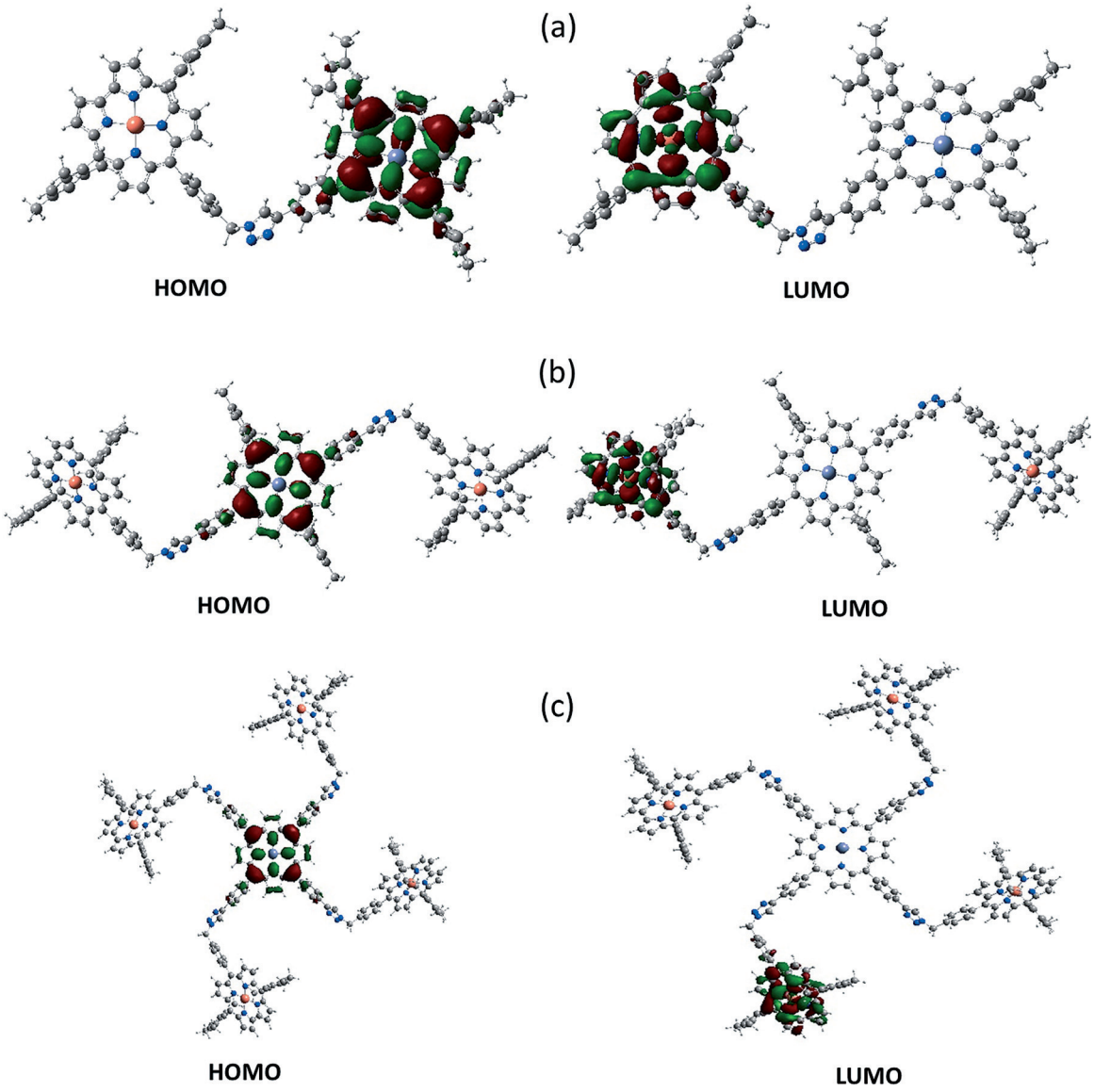

Figure 5. Frontier HOMO and LUMOs of the optimized structures of a) ZnP–CuC, b) ZnP–$(CuC)_2$, and c) ZnP–$(CuC)_4$ conjugates.

In agreement with the electrochemical and spectroelectrochemical results, the HOMO was found to be on the ZnP entity whereas the LUMO was on the CuC entity of the conjugates, establishing them to be the electron-donor and electron-acceptor entities within a given conjugate.

By using the Rehm–Weller approach, free-energy calculations for charge-recombination (ΔG_{CR}) and charge-separation (ΔG_{CS}) processes were calculated according to Equations (1) and (2):[46]

$$-\Delta G_{CR} = (E_{ox} - E_{red}) + \Delta G_S \quad (1)$$

$$-\Delta G_{CS} = \Delta E_{00} - (-\Delta G_{CR}) \quad (2)$$

where ΔG_{CR} and ΔG_{CS} are, respectively, the free-energy changes for charge recombination and charge separation, and ΔE_{00} corresponds to the singlet state energy of ZnP (2.04 eV). E_{ox} and E_{red} are the oxidation potentials of the electron donor ZnP, and the reduction potential of the electron acceptor CuC, respectively. ΔG_S refers to the static energy, calculated by using the 'dielectric continuum model' according to Equation (3):

$$-\Delta G_S = e^2/4\pi\varepsilon_0[(1/2R_+ + 1/2R_- - 1/R_{CC})\Delta(1/\varepsilon_s) \quad (3)$$

where R_+ and R_- refer to the radii of the radical cation and radical anion species, respectively. R_{CC} is the center-to-center distance between the donor and acceptor entities from the optimized structures. ε_0 and ε_s refer to the vacuum permittivity and dielectric constant of the solvents, respectively. These calculations lead to $\Delta G_{CS} = -1.20$ eV and $\Delta G_{CR} = -0.84$ eV in benzonitrile. The large negative ΔG_{CS} values suggest that photoinduced electron transfer is thermodynamically possible in these conjugates.

An energy level diagram depicting different photochemical events in the ZnP–CuC dyad is shown in Figure 6. Based on similarities in the energies of different processes, similar diagrams can be envisioned for the triad and pentad. In the diagram, excitation of ZnP produces ^{1}ZnP*, which could undergo

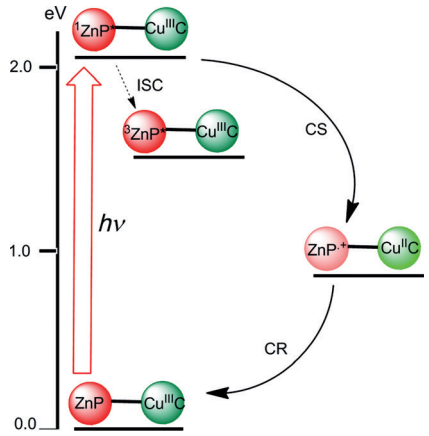

Figure 6. Energy level diagram showing the different photochemical events occurring in the ZnP–CuC dyad in benzonitrile. Energies of the different states were evaluated from spectral and electrochemical studies. Solid arrows indicate major photo-processes, dashed arrow indicates minor photo-processes. ISC = intersystem crossing, CS = charge separation, and CR = charge recombination.

intersystem crossing (ISC) to populate the triplet state of ZnP (^{3}ZnP*) or, alternatively, could undergo energy or electron transfer involving the covalently linked CuC. Owing to the poor spectral overlap between ZnP fluorescence and CuC absorption spectra, singlet energy transfer can be considered a minor process, although this is difficult to confirm owing to the non-emissive nature of CuC. Photoinduced electron transfer from ^{1}ZnP* to CuC is energetically a highly favored process ($\Delta G_{CS} = -1.20$ eV) that would lead to the formation of a ZnP$^{\bullet+}$–Cu^{II}C species. The energy level of the ZnP$^{\bullet+}$–Cu^{II}C species (−0.84 eV) is much lower than that of ^{3}ZnP* (1.50 eV). Our attempts to obtain the phosphorescence spectrum of CuC at 77 K in various glass forming solvents was not successful. Based on the ^{3}MC* and ^{3}MP* energy levels of corrole and porphyrin systems (1.4–1.6 eV), we assume that the energy level of ^{3}CuC* is higher than that of the charge-separated state (> 1 eV). In that case, the ZnP$^{\bullet+}$–Cu^{II}C species would directly charge recombine to yield the ground state ZnP–CuC dyad. To verify this mechanism and to evaluate the kinetics of these processes, femtosecond transient spectral studies were systematically performed and are discussed in the next section.

Femtosecond transient absorption studies

First, femtosecond transient spectral characterization of the control compounds, ZnP and CuC, was performed. As shown in Figure 7a, excitation of ZnP revealed peaks corresponding to S_0–S_n transitions with peak maxima at 458, 581, 625, and 1280 nm, and minima at 560, 600, and 663 nm owing to ground state depletion. The latter two peaks also contained contributions from stimulated emission. The singlet peaks decayed in intensity over time with the appearance of new transient peaks at 474 and 850 nm, corresponding to a triplet state population of ZnP as a result of intersystem crossing (see figure inset for the time profile of the 850 nm peak). As shown in the figure inset, the 1280 nm peak decayed at a rate of 6.03×10^8 s^{-1}, yielding a time constant of 1.7 ns, in agreement with the lifetime of ZnP in benzonitrile. The nanosecond transient absorption spectra of ZnP further revealed peaks resulting from the anticipated triplet state of ZnP at 474, 750, and 850 nm (Figure 7b). As shown in the figure inset, ^{3}ZnP* decayed with a lifetime of about 77 μs.

The femtosecond transient spectra of CuC revealed spectral features of instantaneously formed but short-lived singlet excited CuC with peak maxima at 667, 609, and 753 nm. The 609 nm peak decayed at a rate greater than 10^{10} s^{-1}, indicating fast intersystem crossing to populate the triplet excited state. This result is consistent with the earlier discussed fluorescence studies, where little or no fluorescence from CuC could be detected. The ^{1}CuC* decays rapidly to populate the ^{3}CuC* state, which has peaks at 450 and 665 nm. As shown in the figure inset, the 667 nm peak corresponding to ^{3}CuC* decayed at a rate of 7.0×10^9 s^{-1}, indicating rapid relaxation of the triplet excited state to the ground state. In summary, both singlet and triplet excited states of CuC are relatively short lived in benzonitrile. Accordingly, nanosecond transient studies on CuC revealed no detectable signal.

The femtosecond transient spectra of ZnP–CuC at different delay times in benzonitrile are shown in Figure 8a. From these data it was possible to confirm charge separation in the dyad leading to formation of the ZnP$^{\bullet+}$–Cu^{II}C species. On a short time scale, peaks corresponding to the singlet excited state of ZnP decayed without populating the ^{3}ZnP* triplet state although new transient peaks in the 610 nm region (corresponding to Cu^{II}C) and a broad peak in the 625–700 nm region (corresponding to the formation of ZnPc$^{\bullet+}$) could clearly be observed, establishing charge separation in the dyad. We observed charge separation from the ^{1}ZnP* state and not from the fast decaying ^{1}CuC* state, although at the excitation wavelength of 400 nm both entities can be excited. At higher delay times, decay of the charge-separated state did not lead to any peaks corresponding to ^{3}ZnP* or ^{3}CuC*, indicating that the charge-recombination process yields directly the ground state dyad. This is consistent with the energy level diagram in Figure 6 where populating ^{3}ZnP* from the low-lying charge-separated state is an uphill process. To evaluate the rate of charge separation, k_{CS}, the decay profile of the near-IR band at 1280 nm was monitored and is shown in Figure 8b. For comparative purposes, the decay profile of pristine ZnP is also shown, revealing the rapid decay of ^{1}ZnP* in the dyad system. The k_{CS} evaluated by using a standard procedure was found to be 1.1×10^{10} s^{-1}, revealing fast charge separation. The decay of the 616 nm peak corresponding to charge recombination was found to be biexponential. The faster decay component had a time constant of about 20 ps and the relatively slower decay component had a time constant of 270 ps. These values result

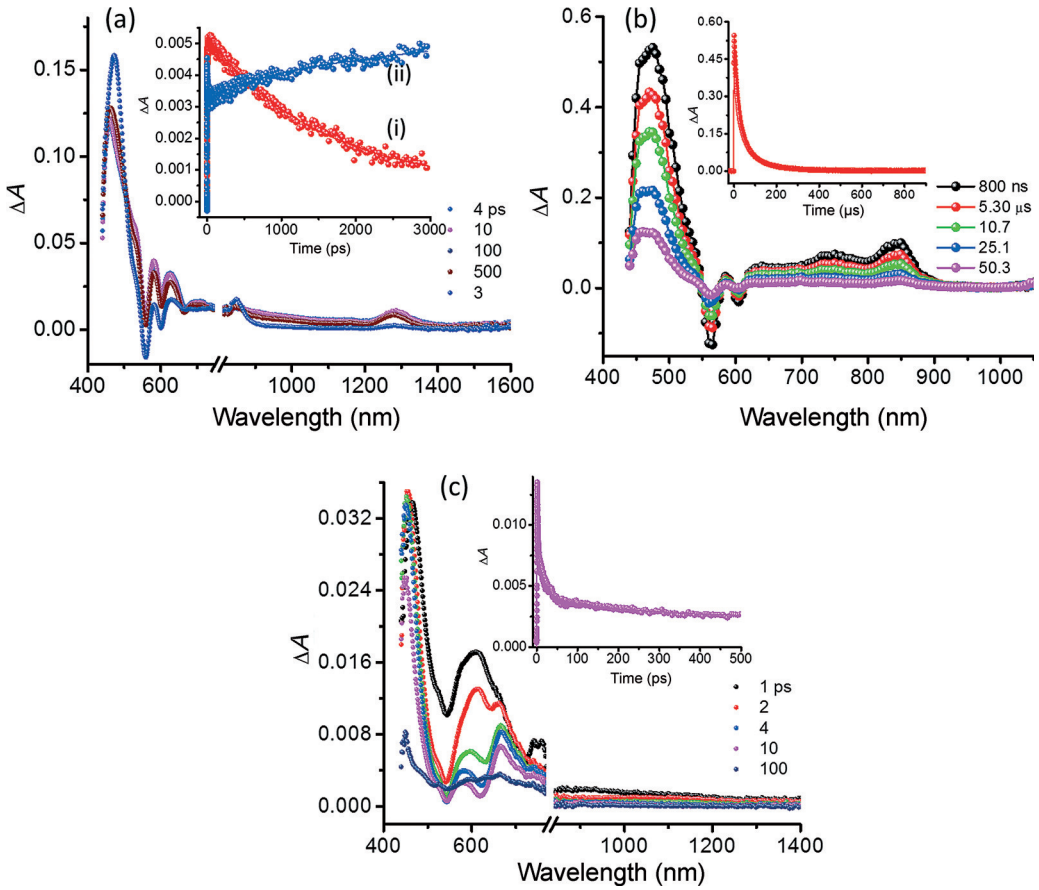

Figure 7. a) Femtosecond transient absorption spectra of ZnP at the indicated delay times (λ_{ex} = 400 nm) in benzonitrile. Figure inset: i) time profile of the 1280 nm peak corresponding to singlet excited ZnP and ii) time profile of the 850 nm peak corresponding to growth of ^{3}ZnP* through intersystem crossing. b) Nanosecond transient absorption spectra of ZnP at the indicated delay times (λ_{ex} = 425 nm) in benzonitrile. Figure inset: time profile of the 474 nm peak. c) Femtosecond transient spectra of CuC at the indicated delay times (λ_{ex} = 400 nm) in benzonitrile. Figure inset: time profile of the 667 nm peak.

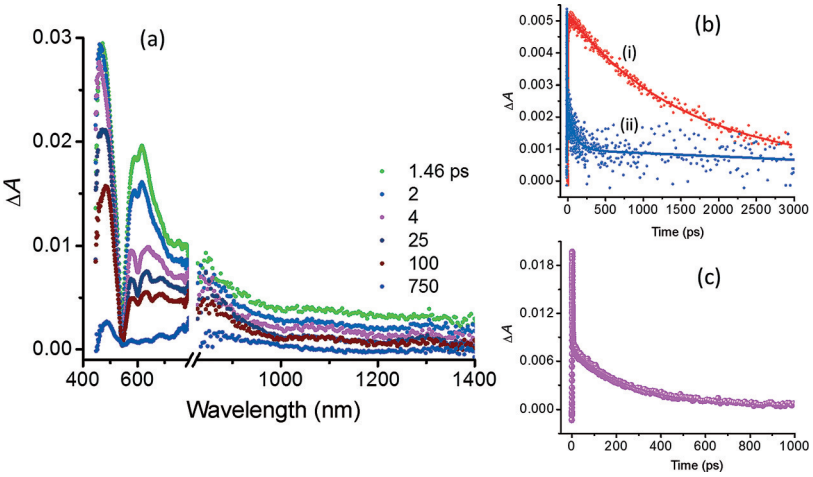

Figure 8. a) Femtosecond transient absorption spectra of the ZnP–CuC dyad at the indicated delay times (λ_{ex} = 400 nm) in benzonitrile. b) Time profile of the 1280 nm peak corresponding to singlet excited ZnP in pristine ZnP (curve i) and in the dyad (curve ii). c) Time profile of the 616 nm peak corresponding to $Cu^{II}C$.

in k_{CR} values of $5.0\times10^{10}\ s^{-1}$ and $3.7\times10^{9}\ s^{-1}$, respectively. However, at the monitoring wavelength of 610 nm, overlapping peaks of the singlet excited state are also present. Hence, the values of k_{CR} reported here should be treated as estimates.

The transient spectral data for the triad and pentad are shown in Figure 9a and b, respectively. In the case of the triad, the spectral features were similar to those of the dyad discussed earlier, with a peak at 610 nm corresponding to $Cu^{II}C$

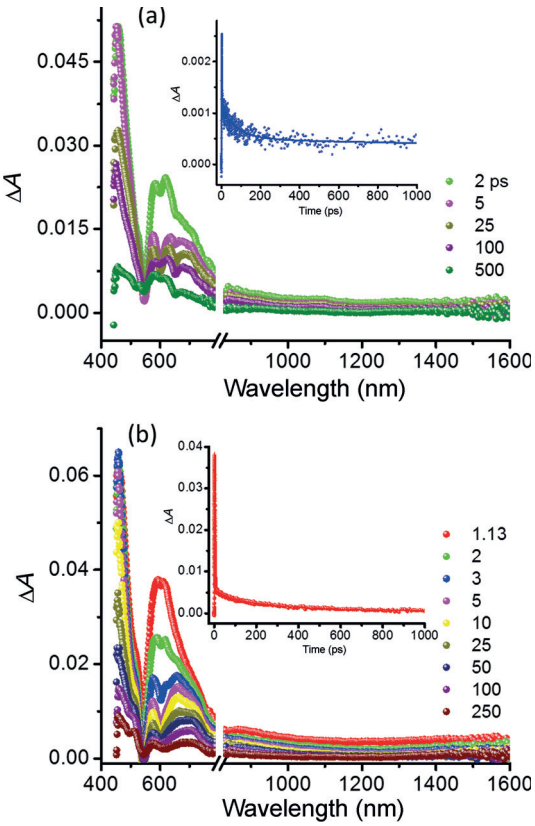

Figure 9. a) Femtosecond transient absorption spectra of the ZnP–$(CuC)_2$ triad at the indicated delay times ($\lambda_{ex}=400$ nm) in benzonitrile. Inset: time profile of the 616 nm peak. b) Transient absorption spectra of the ZnP–$(CuC)_4$ pentad at the indicated delay times ($\lambda_{ex}=400$ nm) in benzonitrile. Inset: time profile of the 616 nm peak.

and features in the 625–700 nm range corresponding to $ZnP^{\bullet+}$, again establishing charge separation in the triad. The k_{CS} determined from the time profile of the 1280 nm band was found to be 1.2×10^{10} s^{-1}, slightly faster than that observed in the case of dyad. The decay of the 610 nm peak corresponding to charge recombination is a biexponential process (see Figure 9a, inset) with the k_{CR} value estimated from the long component being around 5×10^{9} s^{-1}.

The spectral features observed for the ZnP–$(CuC)_4$ pentad (Figure 9b) are also supportive of charge separation but, owing to the presence of four CuC entities, the intensities of the peaks corresponding to the charge-separated species were minimal. Also, the 1280 nm peak of ^{1}ZnP* was too low in intensity for its use in the calculation of k_{CS}, so a rate greater than those calculated in the cases of the dyad and triad is expected. The same could be said for k_{CR} (see Figure 9b, inset, for the time profile of the 610 nm peak), where the decay corresponding to $Cu^{II}C$ was very rapid. Hence, although charge separation is evident, values of k_{CR} and k_{CR} cannot be reported here for the pentad.

Conclusion

The synthesis of a series of donor–acceptor conjugates based on zinc porphyrin as the electron donor and copper(III) corrole as the electron acceptor has been successfully accomplished with outstanding yields. Electrochemical and computational studies revealed the electron-deficient nature of the copper(III) corrole in the conjugates in terms of facile reduction and the locations of the LUMO orbitals. Free-energy calculations were suggestive of the occurrence of photoinduced electron transfer from the singlet excited zinc porphyrin to copper corrole and, accordingly, steady-state fluorescence studies revealed almost complete quenching of ZnP fluorescence in the conjugates. The oxidized and reduced products of the conjugates were characterized spectroelectrochemically and used in the interpretation of transient spectral data from femtosecond transient measurements. The energy level diagram, established by using the spectroscopic, electrochemical, and computational data, predicts the occurrence of charge separation from ^{1}ZnP*, and indicates that the charge-separated state relaxes directly to the ground state during the charge-recombination process. Proof for charge separation was obtained from femtosecond transient spectroscopic studies as it was possible to spectrally characterize the existence of $ZnP^{\bullet+}$ and $Cu^{II}C$ species. The k_{CS} determined for the conjugates were of the order of 10^{10} s^{-1}, revealing ultrafast charge separation. These studies illustrate the importance of copper(III) corrole as a potent electron acceptor for the construction of energy-harvesting model compounds, and constitute the first definitive proof of charge separation in ZnP–$Cu^{III}C$ systems.

Experimental Section

General

Solvents and reagents were obtained from Aldrich Chemicals (Milwaukee, WI), Tokyo Kasei Chemical Co. Ltd. (TCI), Fischer Chemicals (Plano, TX), or Wako Chemical Co. Ltd. Tetra-*n*-butylammonium perchlorate, $(nBu_4N)ClO_4$ used in electrochemical studies was obtained from Fluka Chemicals (Ronkonkoma, NY). NMR spectra were acquired by using a JEOL BX300 spectrometer and chemical shifts (δ) are reported in parts per million (ppm) relative to tetramethylsilane. ESI mass spectra were measured by using a MaXis (Bruker Daltonics, Bremen, Germany) mass spectrometer equipped with a time-of-flight (TOF) analyzer. Mass spectra were measured by using a Shimadzu Axima *CFR*+ spectrometer using dithranol as the matrix. Infrared spectra were measured by using a Thermo-Nicolet 760X FTIR spectrophotometer from samples deposited on a barium fluoride disc from dichloromethane solution followed by drying in air. Electron spin resonance spectra were measured at room temperature from solutions of the compounds in dichloromethane by using a JEOL JES-FA-200 X-band ESR spectrometer.

Synthesis of ZnP–CuC donor–acceptor conjugates

Four different methods were used in the optimization of the synthesis of dyad **5**, triad **6**, and pentad **7**. Typical procedures are given for dyad **5** with corresponding procedures for **6** and **7** given in the Supporting Information.

Method (a): CuI (2 mg, 1.05×10^{-5} mol) was added to a solution of porphyrin **2** (10 mg, 9.63×10^{-6} mol, 1 equiv) and corrole **1** (7 mg, 9.64×10^{-6} mol) in dry dichloromethane (3 mL) and acetonitrile (0.5 mL). The reaction mixture was stirred under an argon atmosphere for 3 d at room temperature. The crude product was purified

by size extrusion chromatography (Biobeads SX-1) eluting with tetrahydrofuran to afford the corrole–porphyrin diconjugate **5** as a brown solid (15 mg, 88%).

Method (b): $CuSO_4 \cdot 5H_2O$ (2 mg, 7.7×10^{-6} mol) and ascorbic acid (1.7 mg, 9.64×10^{-6} mol) were added to a solution of porphyrin **2** (10 mg, 9.63×10^{-6} mol, 1 equiv) and corrole **1** (7 mg, 9.64×10^{-6} mol, 1 equiv) in dry DMF (3 mL) under an argon atmosphere. After stirring for 3 d at 50 °C, the reaction mixture was partitioned between dichloromethane (20 mL) and H_2O (20 mL) and the layers separated. The organic layer was washed with H_2O (3×20 mL), dried over Na_2SO_4, and the solvent removed under reduced pressure. The crude product was purified by size extrusion chromatography (Biobeads SX-1) eluting with tetrahydrofuran to afford the corrole–porphyrin diconjugate **5** as a brown solid (16 mg, 94%).

Method (c): CuI (1 mg, 5.25×10^{-6} mol, 0.5 equiv), *N*,*N*-diisopropylethylamine (DIPEA, 1 mg, 7.74×10^{-6} mol) and acetic acid (1 mg, 1.67×10^{-5} mol) were added to a solution of porphyrin **2** (10 mg, 9.63×10^{-6} mol, 1 equiv) and corrole **1** (7 mg, 9.64×10^{-6} mol) in dry dichloromethane (3 mL). The reaction mixture was stirred for 1 d at RT. The crude product was purified by size extrusion chromatography (Biobeads SX-1) eluting with tetrahydrofuran to afford the corrole–porphyrin diconjugate **5** as a brown solid (17 mg, quant.).

Method (d): A solution of azidocorrole **1** (18.1 mg, 2.72×10^{-5} mol), porphyrin **2** (26 mg, 2.5×10^{-5} mol), and $[Cu(CH_3CN)_4]PF_6$ (12 mg, 3.26×10^{-5} mol) in CH_2Cl_2 (4 mL) was stirred at 80 °C under a N_2 atmosphere. The reaction was monitored by TLC. After completion, water (20 mL) was added and the mixture was extracted with dichloromethane (3×20 mL). The combined organic phases were dried over Na_2SO_4 and the solvent was evaporated under reduced pressure. The crude product was purified by size extrusion chromatography (Biobeads SX-1) eluting with chloroform to afford dyad **5** as a brown solid (44 mg, quant.).

Dyad 5: ^{1}H NMR (300 MHz, $CDCl_3$, 25 °C, TMS): $\delta = 9.00$ (m, 8H, $H_{\beta'}$), 8.29 (d, $^3J(H,H) = 7.7$ Hz, 2H, H_{ar}), 8.20 (d, $^3J(H,H) = 7.7$ Hz, 2H, H_{ar}), 8.09 (s, 6H, H_C), 7.98 (s_{br}, 3H, $H_D + H_{\beta'}$), 7.79 (s, 3H, H_A), 7.66 (d, $^3J(H,H) = 7.5$ Hz, 2H, H_{ar}), 7.53 (d, $^3J(H,H) = 7.4$ Hz, 2H, H_{ar}), 7.35 (s_{br}, 2H, H_β), 7.25 (s_{br}, 2H, H_β), 7.14 (d, $^3J(H,H) = 4.4$ Hz, 2H, H_β), 7.03 (s, 4H, H_G), 5.79 (s, 2H, H_E), 2.39 (s, 6H, H_H), 2.07 (s, 12H, H_F), 1.52 ppm (s, 54H, H_B); ^{13}C NMR (75 MHz, $CDCl_3$, 25 °C, TMS): $\delta = 150.51$, 150.44, 149.99, 148.78, 148.56, 148.47, 143.12, 141.85, 137.64, 135.23, 134.85 (CH), 132.25 (CH), 132.24 (CH), 132.16 (CH), 131.54 (CH), 129.64 (CH), 129.59 (CH), 128.19 (CH), 127.68 (CH), 123.97(CH), 122.63 (CH), 122.49, 121.09 (CH), 120.81 (CH), 120.06, 119.98, 77.20, 54.09 (CH_2), 35.05, 31.77 (CH_3), 29.70, 21.19 (CH_3), 19.78 ppm (CH_3); MS (ESI): calcd: 1761.77; found: 1761.76.

Triad 6: ^{1}H NMR (300 MHz, $CDCl_3$, 25 °C, TMS): $\delta = 8.91$ (d, $^3J(H,H) = 4.5$ Hz, 4H, $H_{\beta'}$), 8.78 (d, $^3J(H,H) = 4.6$ Hz, 4H, $H_{\beta'}$), 8.29 (d, $^3J(H,H) = 7.7$ Hz, 4H, H_{ar}), 8.18 (d, $^3J(H,H) = 7.5$ Hz, 4H, H_{ar}), 8.02 (s_{br}, 6H, $H_E + H_\beta$), 7.65 (d, $^3J(H,H) = 7.9$ Hz, 4H, H_{ar}), 7.51 (d, $^3J(H,H) = 7.6$ Hz, 4H, H_{ar}), 7.35 (s, 4H, H_β), 7.27 (s, 4H, H_G), 7.23 (s_{br}, 4H, H_β), 7.14 (s_{br}, 4H, H_β), 7.02 (s_{br}, 8H, H_B), 5.77 (s, 4H, H_D), 2.62 (s, 6H, H_H), 2.39 (s, 12H, H_A), 2.07 (s, 24H, H_C), 1.83 ppm (s, 12H, H_F); ^{13}C NMR (75 MHz, $CDCl_3$, 25 °C, TMS): $\delta = 150.02$, 148.79, 148.44, 144.02, 143.68, 142.94, 139.25, 139.00, 137.65, 137.48, 135.26 (CH), 134.96, 132.22 (CH), 131.63 (CH), 130.87, 129.68, 128.19 (CH), 127.67 (CH), 124.01 (CH), 121.06, 120.02 (CH), 77.20 (CH), 54.10 (CH_2), 29.71 (CH_2), 21.62 (CH_3), 21.44 (CH_3), 21.18 (CH_3), 19.77 ppm (CH_3); MS (ESI): calcd: 2258.72; found: 2259.71.

Pentad 7: ^{1}H NMR (300 MHz, $CDCl_3$, 25 °C, TMS): $\delta = 8.98$ (s_{br}, 4H, H_E), 8.23 (s_{br}, 8H, H_{ar}), 7.97 (s_{br}, 8H, H_β), 7.65 (s_{br}, 8H, H_{ar}), 7.51 (s_{br}, 8H, H_{ar}), 7.34 (s_{br}, 8H, H_β), 7.30 (s_{br}, 8H, H_{ar}), 7.26 (s_{br}, 8H, H_{ar}), 7.20–7.15 (m, 16H, H_β), 7.00 (s, 16H, H_B), 5.78 (s, 8H, H_D), 2.37 (s, 24H, H_A), 2.05 ppm (s, 48H, H_C); ^{13}C NMR (75 MHz, $CDCl_3$, 25 °C, TMS): $\delta = 150.14$, 148.78, 148.26, 144.17, 143.62, 142.72, 138.26 (CH), 137.61, 135.16/135.14 (CH), 134.87, 132.03 (CH), 131.38 (CH), 129.71 (CH), 128.15 (CH), 127.54 (CH), 123.95, 121.14 (CH), 120.71, 120.01, 77.20, 54.00 (CH_2), 21.18 (CH_3), 19.77 ppm (CH_3); MS (ESI): calcd: 3677.09; found: 3679.12 [*M*+2H]; MALDI-TOF-MS (dithranol): found: 3675.84 [*M*−H].

Spectrophotometric and electrochemical studies

Electronic absorption spectra were measured by using a Shimadzu Model 2550 double monochromator UV/Vis spectrophotometer or a JASCO V-570 UV/Vis/NIR spectrophotometer. Differential pulse voltammograms (DPVs) were recorded by using an EG&G Model 263A potentiostat with a three-electrode system. A platinum button electrode was used as the working electrode. A platinum wire served as the counter electrode and an Ag/AgCl electrode was used as the reference. The ferrocene/ferrocenium redox couple was used as an internal standard. All the solutions were purged prior to electrochemical and spectral measurements by using argon gas. The spectroelectrochemical study was performed by using a cell assembly (SEC-C) supplied by ALS Co., Ltd. (Tokyo, Japan). This assembly comprised a Pt counter electrode, a 6 mm Pt gauze working electrode, and an Ag/AgCl reference electrode in a 1.0 mm path length quartz cell. The optical transmission was limited to 6 mm covering the Pt gauze working electrode.

Computational studies

Computational geometry optimizations were performed by using the B3LYP functional and a mixed basis set (H and C(6–31G), N and O(6–31G(d), and Cu and Zn(6–31G(df)) using the Gaussian 09 software package.[43] The copper corrole and zinc porphyrin structures were first optimized and these structures were used to construct the combined conjugates. The GaussView program of Gaussian was used to generate the frontier HOMO and LUMO orbitals.

Femtosecond laser flash photolysis

Femtosecond transient absorption spectroscopy experiments were performed by using an Ultrafast Femtosecond Laser Source (Libra) by Coherent incorporating a diode-pumped, mode-locked Ti:Sapphire laser (Vitesse) and diode-pumped intracavity-doubled Nd:YLF laser (Evolution) to generate a compressed laser output of 1.45 W. For optical detection, a Helios transient absorption spectrometer coupled with femtosecond harmonics generator, both provided by Ultrafast Systems LLC, was used. The source for the pump and probe pulses was derived from the fundamental output of Libra (Compressed output 1.45 W, pulse width 100 fs) at a repetition rate of 1 kHz. 95% of the fundamental output of the laser was introduced into a harmonic generator, which produces second and third harmonics of 400 and 267 nm in addition to the fundamental 800 nm for excitation, whereas the rest of the output was used for generation of a white light continuum. In the present study, the second harmonic 400 nm excitation pump was used in all the experiments. Kinetic traces at appropriate wavelengths were assembled from the time-resolved spectral data. Data analysis was performed by using Surface Xplorer software supplied by Ultrafast Systems. All measurements were conducted in degassed solutions at 298 K.

Nanosecond laser flash photolysis

The compounds studied were excited by using an Opolette HE 355 LD pumped by a high energy Nd:YAG laser with second and third harmonics OPO (tuning range 410–2200 nm, pulse repetition rate 20 Hz, pulse length 7 ns) with power of 1.0 to 3 mJ per pulse. Transient absorption measurements were performed by using a Proteus UV/Vis/NIR flash photolysis spectrometer (Ultrafast Systems, Sarasota, FL) with a fibre optic delivered white probe light and either a fast rise Si photodiode detector covering the 200–1000 nm range or an InGaAs photodiode detector covering the 900–1600 nm range. The outputs from the photodiodes and a photomultiplier tube were recorded by using a digitizing Tektronix oscilloscope.

Acknowledgements

The authors thank the International Center for Young Scientists (ICYS) for continuing support (THN). This work was partly supported by the World Premier International Research Center Initiative (WPI Initiative), MEXT, Japan. The authors are also grateful to the US National Science Foundation (Grant No. 1401188 to F.D.) for support of this work. The computational work was performed at the Holland Computing Center of the University of Nebraska. We are grateful to Prof. Wouter Maes and Dr. Julija Kudrjasova for fruitful discussions and purification of the conjugates.

Keywords: copper(III) corroles · electron transfer · porphyrins · supramolecular chemistry

[1] a) N. S. Lewis, D. G. Nocera, *Proc. Natl. Acad. Sci. USA* **2006**, *103*, 15729 – 15735; b) P. V. Kamat, *J. Phys. Chem. C* **2007**, *111*, 2834 – 2860; c) T. Umeyama, H. Imahori, *Energy Environ. Sci.* **2008**, *1*, 120 – 133; d) T. Hasobe, *Phys. Chem. Chem. Phys.* **2010**, *12*, 44 – 57; e) V. Balzani, A. Credi, M. Venturi, *ChemSusChem* **2008**, *1*, 26 – 58.

[2] a) *Energy Harvesting Materials*, (Ed.: D. L. Andrews), World Scientific, Singapore, **2005**; b) M. R. Wasielewski, *Acc. Chem. Res.* **2009**, *42*, 1910 – 1921; c) D. Gust, T. A. Moore, A. L. Moore, *Acc. Chem. Res.* **2009**, *42*, 1890 – 1898; d) J. L. Sessler, C. M. Lawrence, J. Jayawickramarajah, *Chem. Soc. Rev.* **2007**, *36*, 314 – 325; e) S. Fukuzumi, K. Ohkubo, *J. Mater. Chem.* **2012**, *22*, 4575 – 4587; f) D. M. Guldi, G. M. A. Rahman, F. Zerbetto, M. Prato, *Acc. Chem. Res.* **2005**, *38*, 871 – 878; g) L. Sánchez, N. Martín, D. M. Guldi, *Angew. Chem. Int. Ed.* **2005**, *44*, 5374 – 5382; *Angew. Chem.* **2005**, *117*, 5508 – 5516; h) S. Fukuzumi, *Phys. Chem. Chem. Phys.* **2008**, *10*, 2283 – 2297; i) M. E. El-Khouly, O. Ito, P. M. Smith, F. D'Souza, *J. Photochem. Photobiol. C* **2004**, *5*, 79 – 104; j) S. Fukuzumi, K. Ohkubo, F. D'Souza, J. L. Sessler, *Chem. Commun.* **2012**, *48*, 9801 – 9815.

[3] *The Porphyrin Handbook* (Eds.: K. M. Kadish, K. M. Smith, R. Guilard), Academic Press, San Diego, **2000**, Vol. 1 – 20.

[4] a) *Phthalocyanine: Properties and Applications* (Eds.: C. C. Leznoff, A. B. P. Lever), VCH, Weinheim, **1993**; b) G. Bottaria, O. Trukhinaa, M. Incea, T. Torres, *Coord. Chem. Rev.* **2012**, *256*, 2453 – 2477; c) A. Satake, Y. Kobuke, *Org. Biomol. Chem.* **2007**, *5*, 1679 – 1691.

[5] a) F. D'Souza, R. Chitta, K. Ohkubo, M. Tasior, N. K. Subbaiyan, M. E. Zandler, M. K. Rogacki, D. T. Gryko, S. Fukuzumi, *J. Am. Chem. Soc.* **2008**, *130*, 14263 – 14272; b) G. Rotas, G. Chralambidis, L. Glatzl, D. T. Gryko, A. Kahnt, A. G. Coutsolelos, N. Tagmatarchis, *Chem. Commun.* **2013**, *49*, 9128 – 9130; c) B. Liu, L. Hongyun, C. Xiaofang, B. Wenting, R. Lipiao, M. Rudolf, F. Plass, L. Fan, X. Lu, D. M. Guldi, *Chem. Eur. J.* **2015**, *21*, 746 – 752; d) C. Li, J. Zhang, Z. Xiujun, Y. Zhou, D. Sun, P. Cheng, B. Zhang, Y. Feng, *RSC Adv.* **2014**, *4*, 40758 – 40762; e) Y. Wang, Z. Wang, X. Guo, R. Cui, X. Gai, S. Yang, F. Chang, J. Dong, B. Sun, *J. Nanosci. Nanotechnol.* **2014**, *14*, 5370 – 5374; f) B. Bursa, D. Wrobel, K. Lewandowska, A. Graja, M. Grzybowski, D. T. Gryko, *Synth. Met.* **2013**, *176*, 18 – 25; g) K. Lewandowska, B. Barszca, J. Wolak, A. Graja, M. Grzybowski, D. T. Gryko, *Dyes Pigm.* **2013**, *96*, 249 – 255; h) K. Sudhakar, S. Gokulnath, L. Giribabu, G. N. Lim, T. Tram, F. D'Souza, *Chem. Asian J.* **2015**, *10*, 2708 – 2719; i) V. Nikolaou, K. Karikis, Y. Farre, G. Charalambidis, F. Odobel, A. G. Coutsolelos, *Dalton Trans.* **2015**, *44*, 13473 – 13479; j) H. L. Buckley, L. K. Rubin, M. Chrominski, B. J. McNicholas, K. H. Y. Tsen, D. T. Gryko, J. Arnold, *Inorg. Chem.* **2014**, *53*, 7941 – 7950.

[6] a) N. Kobayashi, R. Kondo, S. Nakajima, T. Osa, *J. Am. Chem. Soc.* **1990**, *112*, 9640 – 9641; b) C. G. Claessens, D. González-Rodriguez, M. S. Rodriguez-Morgade, A. Medina, T. Torres, *Chem. Rev.* **2014**, *114*, 2192 – 2277; c) C. B. KC, G. N. Lim, F. D'Souza, *Angew. Chem. Int. Ed.* **2015**, *54*, 5088 – 5092; *Angew. Chem.* **2015**, *127*, 5177 – 5181; d) M. Rudolf, O. Trukhina, J. Perles, L. Feng, T. Akasaka, T. Torres, D. M. Guldi, *Chem. Sci.* **2015**, *6*, 4141 – 4147.

[7] a) G. Ulrich, R. Ziessel, A. Harriman, *Angew. Chem. Int. Ed.* **2008**, *47*, 1184 – 1201; *Angew. Chem.* **2008**, *120*, 1202 – 1219; b) M. El-Khouly, S. Fukuzumi, F. D'Souza, *ChemPhysChem* **2014**, *15*, 30 – 47; c) J.-Y. Liu, Y. Huang, R. Menting, B. Röder, E. A. Ermilov, D. K. P. Ng, *Chem. Commun.* **2013**, *49*, 2998 – 3000; d) C. B. KC, G. N. Lim, V. N. Nesterov, P. A. Karr, F. D'Souza, *Chem. Eur. J.* **2014**, *20*, 17100 – 17112.

[8] M. Fujitsuka, *Chem. Asian J.* **2015**, *10*, 2320 – 2326, and references therein.

[9] a) V. Bandi, S. K. Das, S. G. Awuah, Y. You, F. D'Souza, *J. Am. Chem. Soc.* **2014**, *136*, 7571 – 7574; b) V. Bandi, H. B. Gobeze, F. D'Souza, *Chem. Eur. J.* **2015**, *21*, 11483 – 11494; c) S. Shao, H. B. Gobeze, P. A. Karr, F. D'Souza, *Chem. Eur. J.* **2015**, *21*, 16005 – 16016, and references therein.

[10] a) I. Aviv-Harel, Z. Gross, *Coord. Chem. Rev.* **2011**, *255*, 717 – 736; b) L. Flamigni, D. T. Gryko, *Chem. Soc. Rev.* **2009**, *38*, 1635 – 1646.

[11] a) I. Luobeznova, L. Simkhovich, I. Goldberg, Z. Gross, *Eur. J. Inorg. Chem.* **2004**, 1724 – 1732; b) Z. Ou, J. Shao, H. Zhao, K. Ohkubo, I. H. Wasbotten, S. Fukuzumi, A. Ghosh, K. M. Kadish, *J. Porphyrins Phthalocyanines* **2004**, *8*, 1236 – 1247; see also ref. [18]

[12] a) Q. Xie, E. Perez-Cordero, L. Echegoyen, *J. Am. Chem. Soc.* **1992**, *114*, 3978 – 3980; b) L. Sánchez, N. Martín, D. M. Guldi, *Angew. Chem. Int. Ed.* **2005**, *44*, 5374 – 5382; *Angew. Chem.* **2005**, *117*, 5508 – 5516; c) D. I. Schuster, K. Li, D. M. Guldi, *C. R. Chemie* **2006**, *9*, 892 – 908; d) F. D'Souza, O. Ito, *Sci. Prog.* **2013**, *96*, 369 – 397; see also ref. [2h].

[13] a) F. D'Souza, *J. Am. Chem. Soc.* **1996**, *118*, 923 – 924; b) J. Dalton, L. R. Milgrom, *J. Chem. Soc. Chem. Commun.* **1979**, 609 – 610; c) F. D'Souza, N. K. Subbaiyan, Y. Xie, J. P. Hill, K. Ariga, K. Ohkubo, S. Fukuzumi, *J. Am. Chem. Soc.* **2009**, *131*, 16138 – 16146; d) Y. Xie, J. P. Hill, A. L. Schumacher, A. S. D. Sandanayaka, Y. Araki, P. A. Karr, J. Labuta, F. D'Souza, O. Ito, C. E. Anson, A. K. Powell, K. Ariga, *J. Phys. Chem. C* **2008**, *112*, 10559 – 10579; e) A. L. Schumacher, A. S. D. Sandanayaka, J. P. Hill, K. Ariga, P. A. Karr, Y. Araki, O. Ito, F. D'Souza, *Chem. Eur. J.* **2007**, *13*, 4628 – 4635.

[14] R. Paolesse, R. K. Pandey, T. P. Forsyth, L. Jaquinod, K. R. Gerzevske, D. J. Nurco, M. O. Senge, S. Licoccia, T. Boschi, K. M. Smith, *J. Am. Chem. Soc.* **1996**, *118*, 3869 – 3882.

[15] R. Paolesse, F. Sagone, A. Macagnano, T. Boschi, L. Prodi, M. Montalti, N. Zaccheroni, F. Bolletta, K. M. Smith, *J. Porphyrins Phthalocyanines* **1999**, *3*, 364 – 370.

[16] C. Chen, Y.-Z. Zhu, Q.-J. Fan, H.-B. Song, J.-Y. Zheng, *Chem. Lett.* **2013**, *41*, 936 – 938.

[17] K. M. Kadish, Z. Ou, J. Shao, C. P. Gros, J. M. Barbe, F. Jerome, F. Bolze, F. Burdet, R. Guilard, *Inorg. Chem.* **2002**, *41*, 3990 – 4005.

[18] R. Guilard, C. P. Gros, J. M. Barbe, E. Espinosa, F. Jerome, A. Tabard, J. M. Latour, J. Shao, Z. Ou, K. M. Kadish, *Inorg. Chem.* **2004**, *43*, 7441 – 7455.

[19] K. M. Kadish, L. Fremond, J. Shen, P. Chen, K. Ohkubo, S. Fukuzumi, M. El Ojaimi, C. P. Gros, J. M. Barbe, R. Guilard, *Inorg. Chem.* **2009**, *48*, 2571 – 2582.

[20] K. M. Kadish, L. Fremond, Z. P. Ou, J. G. Shao, C. N. Shi, F. C. Anson, F. Burdet, C. P. Gros, J. M. Barbe, R. Guilard, *J. Am. Chem. Soc.* **2005**, *127*, 5625 – 5631.

[21] K. M. Kadish, J. Shao, Z. Ou, L. Fremond, R. Zhan, F. Burdet, J. M. Barbe, C. P. Gros, R. Guilard, *Inorg. Chem.* **2005**, *44*, 6744 – 6754.

[22] K. M. Kadish, J. Shao, Z. Ou, R. Zhan, F. Burdet, J. M. Barbe, C. P. Gros, R. Guilard, *Inorg. Chem.* **2005**, *44*, 9023 – 9038.

[23] R. Guilard, F. Burdet, J. M. Barbe, C. P. Gros, E. Espinosa, J. Shao, Z. Ou, R. Zhan, K. M. Kadish, *Inorg. Chem.* **2005**, *44*, 3972 – 3983.

[24] C. P. Gros, F. Brisach, A. Meristoudi, E. Espinosa, R. Guilard, P. D. Harvey, *Inorg. Chem.* **2007**, *46*, 125 – 135.

[25] J. M. Barbe, F. Burdet, E. Espinosa, C. P. Gros, R. Guilard, *J. Porphyrins Phthalocyanines* **2003**, *7*, 365 – 374.
[26] F. Jerome, C. P. Gros, C. Tardieux, J.-M. Barbe, R. Guilard, *New J. Chem.* **1998**, *22*, 1327 – 1329.
[27] S. Hiroto, I. Hisaki, H. Shinokubo, A. Osuka, *Angew. Chem. Int. Ed.* **2005**, *44*, 6763 – 6766; *Angew. Chem.* **2005**, *117*, 6921 – 6924.
[28] A. I. Ciuciu, L. Flamigni, R. Voloshchuk, D. T. Gryko, *Chem. Asian J.* **2013**, *8*, 1004 – 1014.
[29] L. Flamigni, B. Ventura, M. Tasior, D. T. Gryko, *Inorg. Chim. Acta* **2007**, *360*, 803 – 813.
[30] T. H. Ngo, F. Nastasi, F. Puntoriero, S. Campagna, W. Dehaen, W. Maes, *Eur. J. Org. Chem.* **2012**, 5605 – 5617.
[31] T. H. Ngo, W. Van Rossom, W. Dehaen, W. Maes, *Org. Biomol. Chem.* **2009**, *7*, 439 – 443.
[32] W. Beenken, M. Presselt, T. H. Ngo, W. Dehaen, W. Maes, M. Kruk, *J. Phys. Chem. A* **2014**, *118*, 862 – 871.
[33] Y. B. Ivanova, V. A. Savva, N. Z. Mamardashvili, A. S. Starukhin, T. H. Ngo, W. Dehaen, W. Maes, M. M. Kruk, *J. Phys. Chem. A* **2012**, *116*, 10683 – 10694.
[34] M. Kruk, T. H. Ngo, V. Savva, A. Starukhin, W. Dehaen, W. Maes, *J. Phys. Chem. A* **2012**, *116*, 10704 – 10711.
[35] M. Kruk, T. H. Ngo, P. Verstappen, A. Starukhin, J. Hofkens, W. Dehaen, W. Maes, *J. Phys. Chem. A* **2012**, *116*, 10695 – 10703.
[36] W. Maes, T. H. Ngo, J. Vanderhaeghen, W. Dehaen, *Org. Lett.* **2007**, *9*, 3165 – 3168.
[37] F. Nastasi, S. Campagna, T. H. Ngo, W. Dehaen, W. Maes, M. Kruk, *Photochem. Photobiol. Sci.* **2011**, *10*, 143 – 150.
[38] T. H. Ngo, F. Puntoriero, F. Nastasi, K. Robeyns, L. Van Meervelt, S. Campagna, W. Dehaen, W. Maes, *Chem. Eur. J.* **2010**, *16*, 5691 – 5705.
[39] N. K. Devaraj, R. A. Decreau, W. Ebina, J. P. Collman, C. E. D. Chidsey, *J. Phys. Chem. B* **2006**, *110*, 15955 – 15962.
[40] L. C. Le Pleux, Y. Pellegrin, E. Blart, F. Odobel, A. Harriman, *J. Phys. Chem. A* **2011**, *115*, 5069 – 5080.
[41] During the course of this work, Nikolaou and co-workers reported a synthesis (also using the click reaction) of a porphyrin–corrole dyad and some of its photophysical and electrochemical properties. They assigned the phenomenon of fluorescence quenching in their dyad as a possible symptom of electron transfer from porphyrin to copper corrole although this was not unequivocally demonstrated. See ref. [5i].
[42] V. V. Rostovtsev, L. G. Green, V. V. Fokin, K. B. Sharpless, *Angew. Chem. Int. Ed.* **2002**, *41*, 2596 – 2599; *Angew. Chem.* **2002**, *114*, 2708 – 2711.
[43] Gaussian 09, Revision D.01, M. J. Frisch, G. W. Trucks, H. B. Schlegel, G. E. Scuseria, M. A. Robb, J. R. Cheeseman, G. Scalmani, V. Barone, B. Mennucci, G. A. Petersson, H. Nakatsuji, M. Caricato, X. Li, H. P. Hratchian, A. F. Izmaylov, J. Bloino, G. Zheng, J. L. Sonnenberg, M. Hada, M. Ehara, K. Toyota, R. Fukuda, J. Hasegawa, M. Ishida, T. Nakajima, Y. Honda, O. Kitao, H. Nakai, T. Vreven, J. A. Montgomery, Jr., J. E. Peralta, F. Ogliaro, M. Bearpark, J. J. Heyd, E. Brothers, K. N. Kudin, V. N. Staroverov, R. Kobayashi, J. Normand, K. Raghavachari, A. Rendell, J. C. Burant, S. S. Iyengar, J. Tomasi, M. Cossi, N. Rega, J. M. Millam, M. Klene, J. E. Knox, J. B. Cross, V. Bakken, C. Adamo, J. Jaramillo, R. Gomperts, R. E. Stratmann, O. Yazyev, A. J. Austin, R. Cammi, C. Pomelli, J. W. Ochterski, R. L. Martin, K. Morokuma, V. G. Zakrzewski, G. A. Voth, P. Salvador, J. J. Dannenberg, S. Dapprich, A. D. Daniels, Ö. Farkas, J. B. Foresman, J. V. Ortiz, J. Cioslowski, and D. J. Fox, Gaussian, Inc., Wallingford CT, **2009**.
[44] C. Shao, X. Wang, J. Xu, J. Zhao, Q. Zhang, Y. Hu, *J. Org. Chem.* **2010**, *75*, 7002 – 7005.
[45] C. Shao, X. Wang, Q. Zhang, S. Luo, J. Zhao, Y. Hu, *J. Org. Chem.* **2011**, *76*, 6832 – 6836.
[46] D. Rehm, A. Weller, *Isr. J. Chem.* **1970**, *8*, 259 – 271.

Received: September 1, 2015
Published online on November 30, 2015